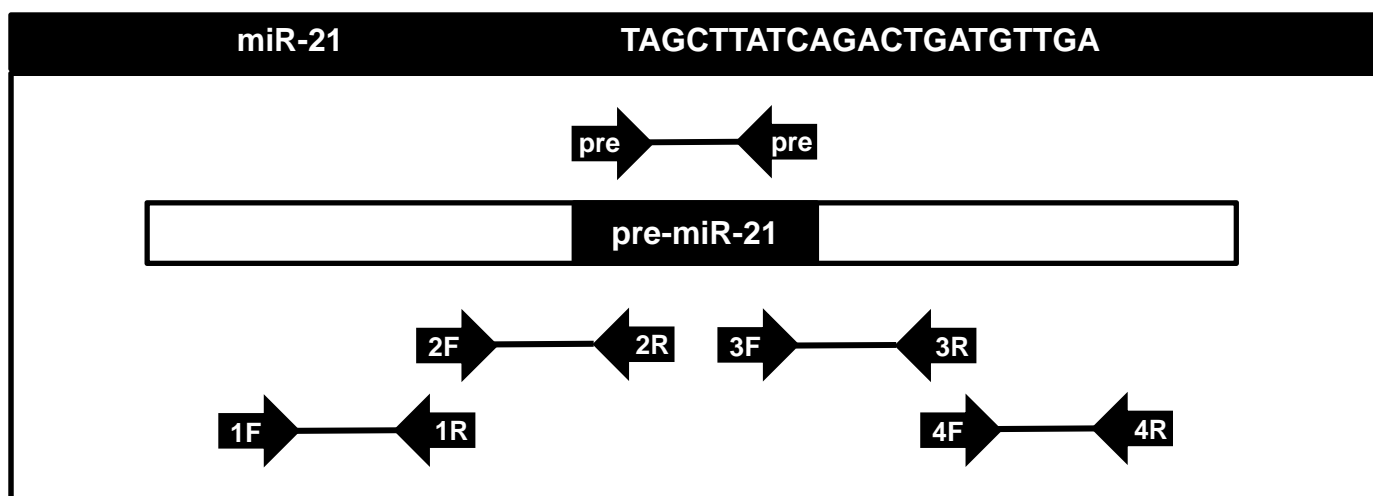


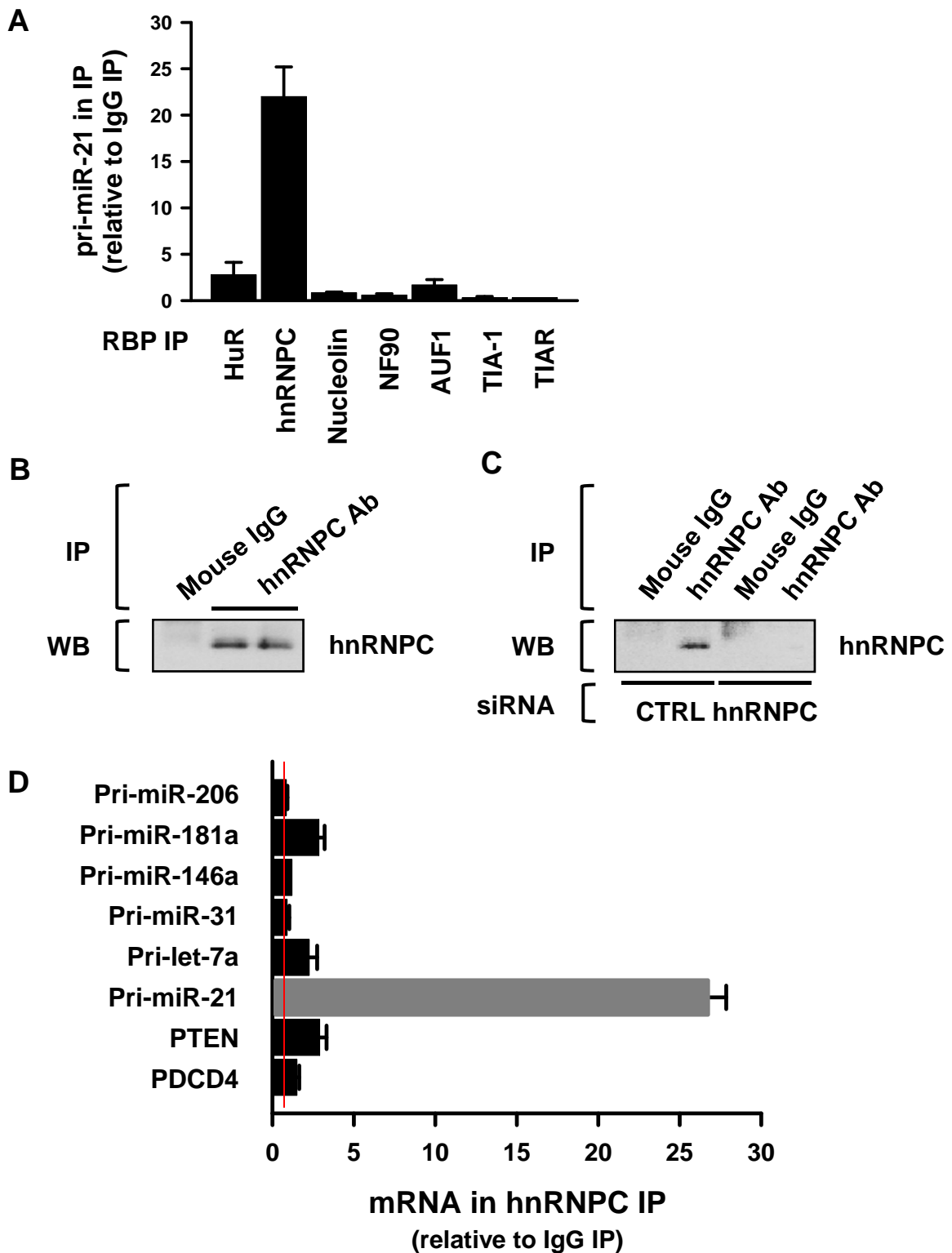
Supplemental figure 1-A. Sequences of primers which are used for miR-21



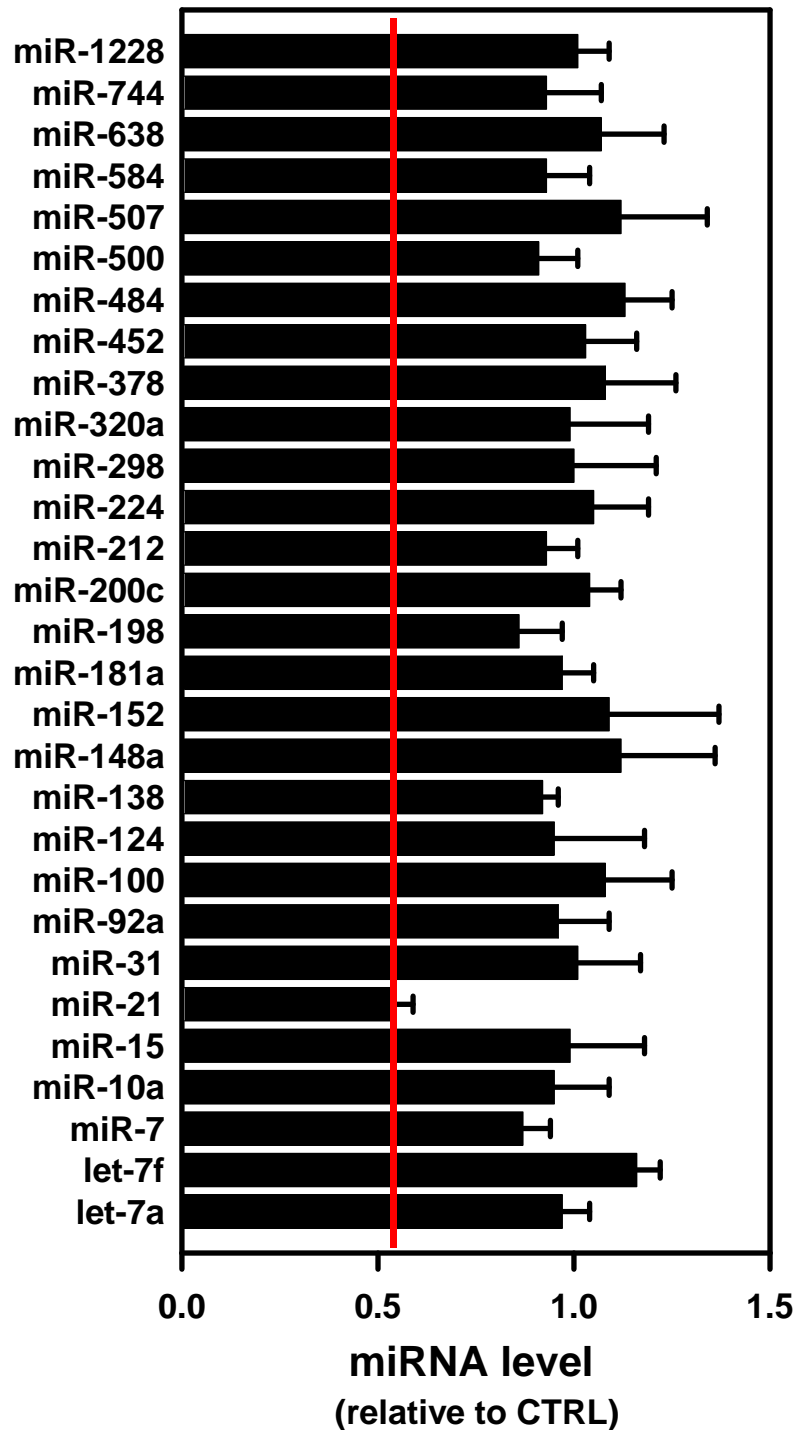
Primer	Forward	Reverse
pre-miR-21	TGTCGGGTAGCTTATCAGAC	TGTACAGACAGCCCATCGACT
pri-miR-21 #1	TTTTGTTTTGCTTGGGAGGA	AAGCAGACAGTCAGGCAGGAT
pri-miR-21 #2	CAAATCCTGCCTGACTGTCTG	ACTGGTGTTGCCATGAGATTC
pri-miR-21 #3	GGGCTGTCTGACATTTTGGT	TCCATAAAATCCTCCCTCCA
pri-miR-21 #4	CATTGTGGGTTTTGAAAAGGTTA	CCACGACTAGAGGCTGACTTAGA

Supplemental figure 1-B. Sequences of primers

Genes	Forward	Reverse
hnRNPC	GGAGATGTACGGGTCAGTAACA	CCCGAGCAATAGGAGGAGGA
PDCD4	GTTGGCAGTATCCTTAGCATTGG	TCCACATCAGTTGTGCTCATT AC
PTEN	ACCGCCAAATTTAATTGCAG	TTCGTCCTTTCCAGCTTTA
GAPDH	TGCACCACCAACTGCTTAGC	GGCATGGACTGTGGTCATGAG

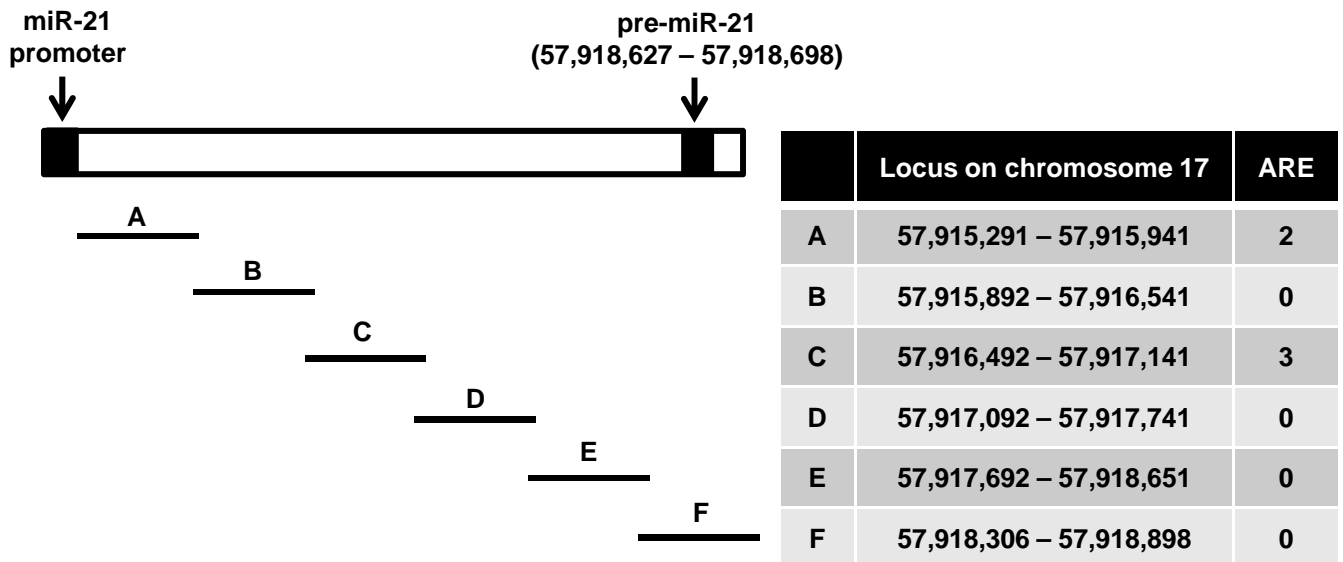


**Supplemental figure 2. IP RNP experiment for RBPs binding to pri-miR-21.** (A) PEB lysates of T98G cells were incubated with each anti-RBP antibody or corresponding IgG. The level of pri-miR-21 in each RBP IP was determined by RT-qPCR analysis. (B,C) To verify IP efficiency, we checked the level of hnRNPC in IP materials obtained from PEB lysates. (D) PEB lysates of T98G cells were incubated with mouse IgG or anti-hnRNPC antibody. The level of several pri-miRNAs, PTEN, and PDCD4 mRNA in hnRNPC IP was determined by RT-qPCR analysis.

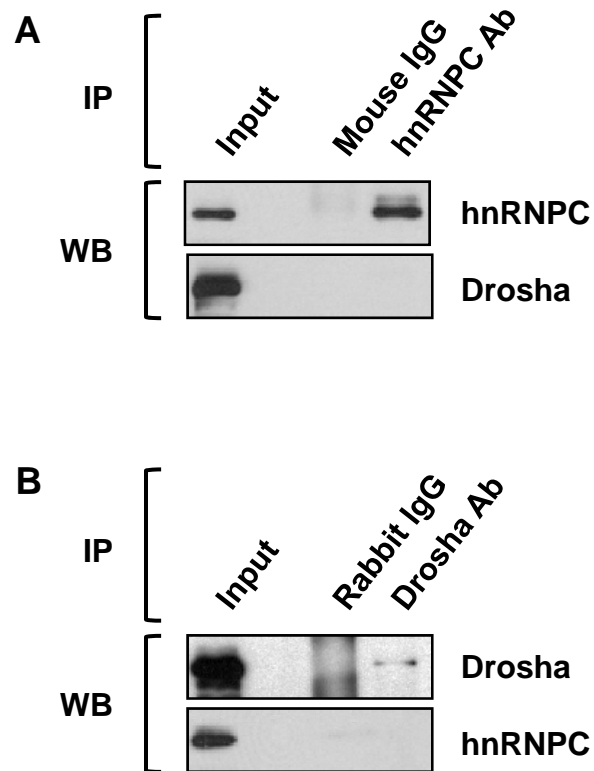


**Supplemental figure 3. Silencing of hnRNPC specifically suppresses miR-21.** T98G cells were transfected with control (CTRL) or hnRNPC siRNA. The level of mature miRNAs was determined by RT-qPCR using QuantiMir miRNA Assay (SBI).

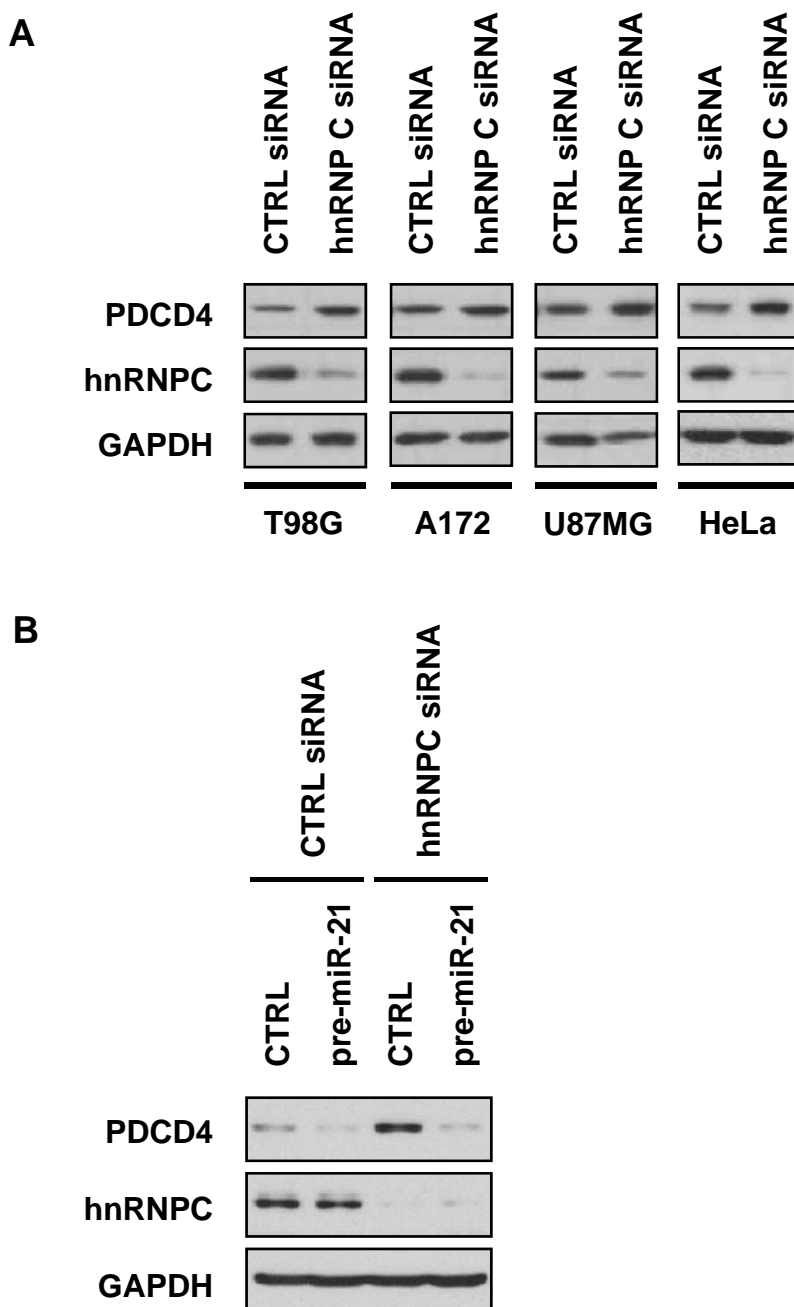
## Park et al., Supplemental figure 4



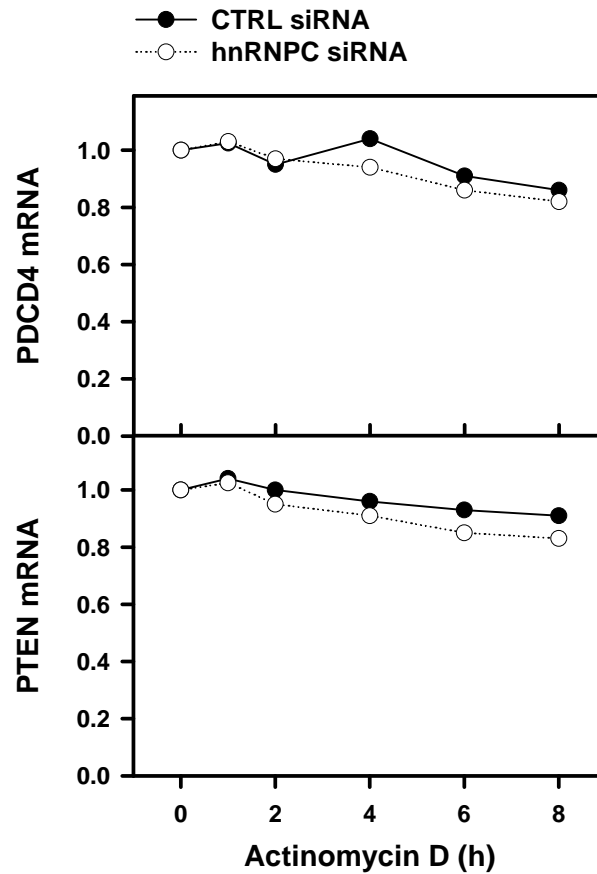
**Supplemental figure 4. Scheme of biotin pull-down assay to identify hnRNPC binding sites in pri-miR-21.** For biotin pull-down analysis, six biotinylated transcripts spanning pri-miR-21 were synthesized using T98G cDNA as template. The number of predicted AU-rich elements (ARE) in each fragment was represented.



**Supplemental figure 5. HnRNPC does not interact directly with Drosha: hnRNPC-mediated miR-21 regulation is independent of Drosha function.** (A) T98G whole-cell lysates were used in co-immunoprecipitation (co-IP) assays with either mouse IgG or anti-hnRNPC antibody, followed by Western blot (WB) detection of hnRNPC and Drosha. (B) Assays were performed as in A except that rabbit IgG or anti-Drosha antibody were used for co-IP.

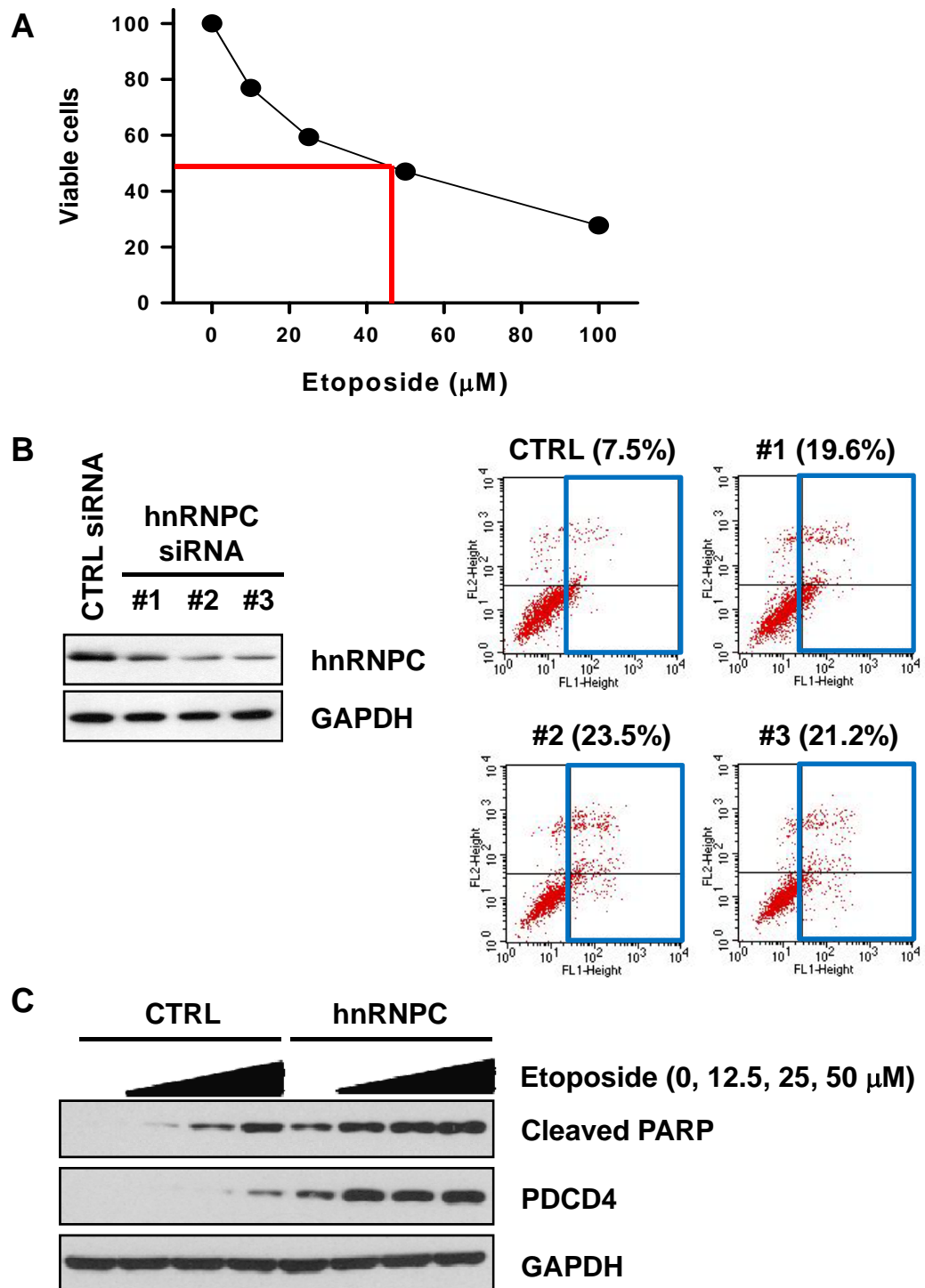


**Supplemental figure 6. PDCD4 expression is increased by hnRNP C silencing in various cells, which is reversed by miR-21 overexpression.** (A) Various glioma cells (T98G, A172, and U87MG) and HeLa cells were transfected with control (CTRL) or hnRNP C siRNA. 48 h later, the expression of PDCD4, hnRNP C, and GAPDH was determined by Western blot analysis. (B) T98G cells were co-transfected with hnRNP C siRNA and pre-miR-21. 48 h later, the expression of PDCD4, hnRNP C, and GAPDH was determined by Western blot analysis.



**Supplemental figure 7. The stability of PDCD4 and PTEN mRNA in control (CTRL) and hnRNPC siRNA-transfected T98G cells.** The stability of PDCD4 and PTEN mRNA was assessed following treatment with transcription inhibitor actinomycin D (1  $\mu$ g/ml) for the time periods indicated. The level of PDCD4 and PTEN mRNA was determined by RT-qPCR analysis.

Park et al., Supplemental figure 8

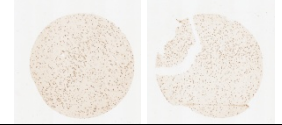


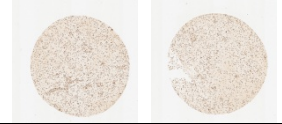

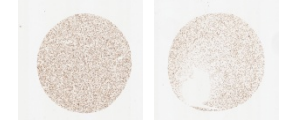

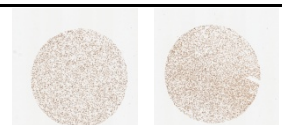

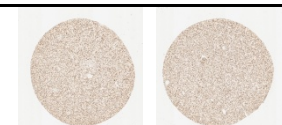

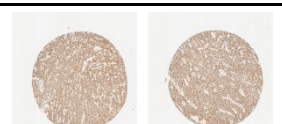


**Supplemental figure 8. Dose response of etoposide-induced apoptosis and enhancement of apoptosis by hnRNPC silencing.** (A) T98G cells were treated with indicated concentrations of etoposide for 24 h and cytotoxicity was determined by MTS assay. (B) Cells were transfected with control (CTRL) or hnRNPC siRNA. 48 h later, the expression of hnRNPC and GAPDH was determined by Western blot analysis. Apoptotic cells were calculated using FACS analysis after staining with annexin V/PI. (C) Transfected cells were treated with indicated concentrations of etoposide for 24 h. The level of cleaved PARP, PDCD4, and GAPDH was determined by Western blot analysis.

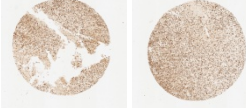
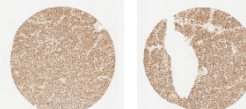
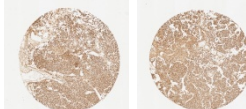
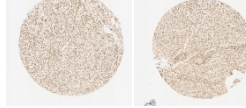
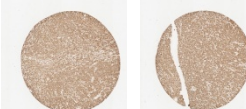
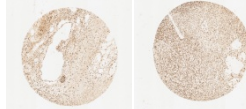
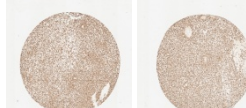
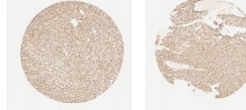
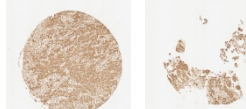
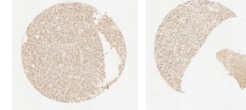
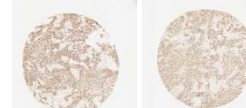
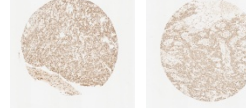


Park et al., Supplemental figure 9-1

Supplemental figure 9. IHC analysis of hnRNPC using TMA of brain tumors

Age / Sex / Anatomic site Pathology / Grade	Stained tissues	Intensity (SD)
58 / M / Cerebral cortex Normal		1.0 (0.35)
58 / M / Cerebra medulla Normal		0.9 (0.08)
58 / M / Cerebellum Normal		1.9 (0.22)
30 / F / Cerebra Astrocytoma / I		1.2 (0.05)
31 / M / Cerebra Astrocytoma / II		1.9 (0.31)
38 / F Cerebra Astrocytoma / II		3.0 (0.14)
35 / M / Cerebra Astrocytoma / II		3.0 (0.06)
24 / M / Cerebra Astrocytoma / II		2.5 (0.27)
47 / M / Cerebra Astrocytoma / II		1.6 (0.09)
37 / F / Cerebra Astrocytoma / II		1.8 (0.21)
55 / F / Cerebra Astrocytoma / II		1.9 (0.12)
15 / F / Cerebra Astrocytoma / II~III		3.3 (0.01)

Supplemental figure 9. Continued

Age / Sex / Anatomic site Pathology / Grade	Stained tissues	Intensity (SD)
71 / M / Cerebra Astrocytoma / II~III		2.2 (0.09)
50 / M / Cerebra Anaplastic astrocytoma / III~IV		3.1 (0.01)
42 / M / Cerebra Anaplastic astrocytoma / III		3.3 (0.07)
52 / F / Cerebra Anaplastic astrocytoma / III		2.4 (0.44)
17 / M / Cerebra Anaplastic astrocytoma / III		3.2 (0.06)
54 / M / Cerebra Anaplastic astrocytoma / III		3.1 (0.30)
7 / M / Cerebra Glioblastoma multiform / III		3.2 (0.11)
66 / M / Cerebra Glioblastoma multiform / IV		2.9 (0.12)
65 / F / Cerebra Glioblastoma multiform / IV		3.2 (0.11)
43 / M / Cerebra Oligodendroglioma / II		2.3 (0.35)
49 / M / Cerebra Ependymoma		2.3 (0.74)
34 / M / Cerebra Ependymoma		2.5 (0.25)